Electrocatalysis

DOI: 10.1002/anie.201203589

Electrochemical Milling and Faceting: Size Reduction and Catalytic Activation of Palladium Nanoparticles**

Yan-Xin Chen, Alessandro Lavacchi, Sheng-Pei Chen, Francesco di Benedetto, Manuela Bevilacqua, Claudio Bianchini, Paolo Fornasiero, Massimo Innocenti, Marcello Marelli, Werner Oberhauser, Shi-Gang Sun,* and Francesco Vizza**

Mastering the size and surface of metal nanoparticles (NPs) is a challenge in catalytic nanotechnology. Outstanding improvements in the material functionality have recently been reported, demonstrating the successful use of tailored NPs in a variety of catalytic processes.[1,2] Some of us have reported on nanostructured palladium for the realization of a new "green" and energetically self-sustainable process, used in the chemical industry and based on the electro-oxidation of renewable alcohols.[3] This discovery is receiving increasing attention from public and private institutions interested in the setup of fossil fuel-free and environmentally friendly processes.[4–6] The oxidation of alcohols and other small organic molecules (SOM) proceeds faster on nanocrystals terminated with high-index facets (HIFs) because of the high density of low-coordinated surface atoms (coordination number < 8).[7] The exploitation of the catalytic properties of the HIFs depends on the availability of methods capable of generating supported NPs with high-index terminations as well as controlling the particle size and metal loading. The contemporaneous control of these parameters is a major challenge of catalytic and electrocatalytic nanotechnology, where the energy efficiency needs to be combined with a low noble-metal loading. For example, although a variety of metal (e.g., Pt, Pd, and Au) NPs with HIFs have been synthesized through electrochemical square wave potential deposition (SWPD) or wet chemistry methods,[8–14] the particle sizes are usually much larger than those of practical catalysts (2–10 nm). As a result, the catalytic activity based on the noble-metal mass is not improved considerably, although the activity in terms of electrochemically active surface area (EASA) can be enhanced several times.

Herein we report a novel method for the modification of metal NPs, denoted as electrochemical milling and faceting (ECMF), by which large Pd NPs (35 nm) of low-index facets supported on TiO_2 can be milled into many small NPs (7 nm) with some HIFs or a high density of step atoms. By this approach, the catalytic activity of supported Pd NPs was enhanced by an order of magnitude for the ethanol electro-oxidation, and was even three times higher than the highest value reported so far. This new approach to the synthesis of HIF-Pd NPs allows us to control the metal loading, particle size, and surface structure, independently from each other.

The three-step procedure to achieve this goal is shown in Figure 1. The first step (Figure 1 A) consists of the deposition of Pd particle onto a high-surface-area support with a desired metal loading. Deposition is followed by a post-deposition treatment which consists of two phases aiming at the reduction of the particle size and generation of HIFs (Figure 1 B,C). Such a post-deposition treatment is the main focus of the present work: it includes milling and faceting actions, both of them achieved through controlled electrode potentials. For this reason, we refer to our method as electrochemical milling and faceting (ECMF).

The selected support was a titania nanotube array (TNTA) obtained by anodization and annealing (see the Experimental Section). The choice of this support was made in view of its robustness to the electrochemical treatment as well as by the possibility to precisely control the TNTA structure (anatase, see Figure S1 in the Supporting Information) and morphology. In particular, nanotubes with a diameter of 80 nm and a length of 2.0 μm have been prepared.

The TNTAs were impregnated with palladium chloride which was then reduced with sodium borohydride (see the Experimental Section for details) to give a metal loading of

[*] Y. X. Chen, Dr. A. Lavacchi, Dr. M. Bevilacqua, Dr. C. Bianchini, Dr. W. Oberhauser, Dr. F. Vizza
ICCOM-CNR, Polo Scientifico Area CNR
Via Madonna del Piano 10, 50019, Sesto Fiorentino, Firenze (Italy)
E-mail: alessandro.lavacchi@iccom.cnr.it
francesco.vizza@iccom.cnr.it
Prof. S. P. Chen, Prof. S. G. Sun
State Key Laboratory of Physical Chemistry of Solid Surfaces
Department of Chemistry
College of Chemistry and Chemical Engineering
Xiamen University, Xiamen, 361005 (China)
E-mail: sgsun@xmu.edu.cn
Dr. F. di Benedetto, Dr. M. Innocenti
University of Firenze, Sesto Fiorentino, Firenze (Italy)
Prof. P. Fornasiero
University of Trieste, Trieste (Italy)
Dr. M. Marelli
ISTM-CNR, Milano (Italy)

[**] Financial support from Ing. Guido Gay (Switzerland) for the project "Conversion of CO_2 in hydrocarbons and oxygenated compounds", from the Ente Cassa di Risparmio Firenze for the HYDROLAB^2 project, from the MIUR (Italy) for the PRIN 2008 project (project number 2008N7CYL5), from the MATTM (Italy) for the PIRODE project (number 94), from the MSE for the PRIT project Industria 2015, and from the Regione Lombardia for the project "ACCORDO QUADRO Regione Lombardia e CNR per l'attuazione di programmi di ricerca e sviluppo" is gratefully acknowledged. S.G.S. and his research group are funded by the Natural Science Foundation of China (grant number 21021002).

Supporting information for this article is available on the WWW under http://dx.doi.org/10.1002/anie.201203589.

© 2012 Wiley-VCH Verlag GmbH & Co. KGaA, Weinheim

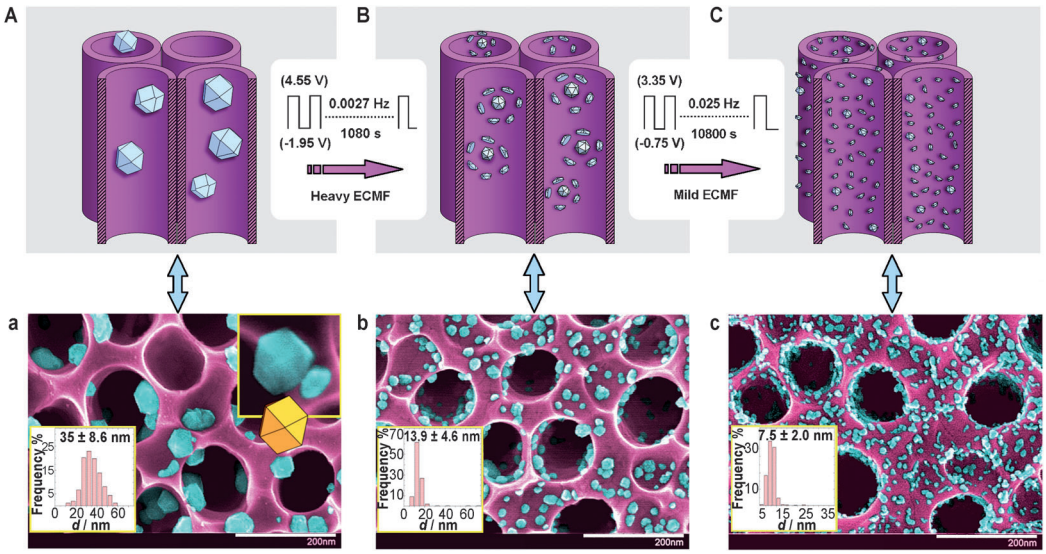

Figure 1. A) TNTAs with as-deposited Pd and a) the corresponding SEM image. B) TNTAs with Pd after heavy ECMF and b) the corresponding SEM image. C) TNTAs with Pd after heavy and mild ECFM and c) the corresponding SEM image. False coloring of the SEM images shows Pd NPs (light blue) and TNTA support (violet). The white scale bars in (a–c) are 200 nm.

22.42 $\mu g\,cm^{-2}$. Scanning electron microscopy (SEM) images of the material obtained showed NPs with an average particle size of 35 nm, with shapes largely exhibiting low-index terminations ({100}, {111}; Figure 1a and Figure S2 in the Supporting Information). An EASA of 4.25 cm^2 was measured for this material (Figure S8). The electro-oxidation of ethanol was investigated by cyclic voltammetry (CV), after stabilization of the peak current density. Relevant electrochemical parameters are listed in Table 1.

The heavy ECMF required a palladium oxidation at 4.55 V (vs. reversible hydrogen electrode, RHE) for 180 s, followed by the reduction of the Pd oxides at −1.95 V (vs. RHE) for 180 s. The whole sequence was repeated three times (Figure 1B). The SEM image of the resulting product (Figure 1b and Figure S3 in the Supporting Information) showed the occurrence of particle fragmentation with an average particle size of 14 nm, whereas the elemental analysis showed a 6.70% metal loss (Table 1). SEM images on the TNTAs without metal loading and subjected to ECMF allowed us to exclude that fragments were originated by the substrate (Figure S6). We have observed by SEM that Pd oxidation alone cannot generate the fragments, resulting exclusively in surface roughening (Figure S7a). According to the literature,[15] Pd roughening may occur with large anodic electrode polarization (> 1.23 V vs. RHE) as a result of the formation of β-oxide islands. X-ray photoelectron spectroscopy (XPS) measurements of the Pd NPs supported on the TNTAs oxidized at 4.55 V (vs. RHE) for 180 s were consistent with β-oxide formation (Figure S11). SEM images in Figure S7b showed that the NPs on the TNTAs, after the treatment, have a size comparable to that of the β-oxide islands. Such an observation suggests that the milling may occur through progressive breaking up the surface layer, possibly caused by the stress generated through the reduction of palladium oxide at a potential low enough to generate a strong hydrogen evolution and absorption. This is the first time that electrochemical milling is observed for palladium. Previous investigations on the production of NPs through cathodic polarization of metal foils where unsuccessful with Pd.[16,17] Further the cathodic polarization method produced unsupported NPs without control of the surface structure which in the ECMF occurs by the repeated oxidation and reduction of the Pd surface.

As shown in Table 1, the peak current density for the oxidation of ethanol on the heavy ECMF Pd-TNTA is five times higher than the density of the as-deposited sample (116 $mA\,cm^{-2}$ vs. 22.1 $mA\,cm^{-2}$), while the ethanol oxidation onset potential is negatively shifted (0.29 vs. 0.38 V). The increase in the EASA (10.4 vs. 4.25 cm^2) cannot entirely account for the current density increase. Hence we ascribe this effect to the activation of the surface, in particular to an increased density of low-coordination surface Pd atoms. To prove this assumption, high-resolution transmission electron microscopy (HRTEM; Figure 3) and CV (Figure 2a) measurements were carried out. The HRTEM image of a Pd nanoparticle removed from the TNTAs showed a typical multiple twinned particle (MTP; Figure 3a). This observation

Table 1: Parameters for the catalytic activity assessment.

Sample	Pd loading [$\mu g\,cm^{-2}$]	EASA[a] [cm^2]	j_p [$mA\,cm^{-2}$]	j_p^{m}[b] [$mA\,\mu g^{-1}$ Pd]	j_p^{EASA} [$mA\,cm^{-2}$]	Onset potential [V vs. RHE]
as-deposited Pd-TNTA	22.42	4.25	22.1	0.99 (0.99)	5.20	0.38
heavy ECMF Pd-TNTA	20.92	10.4	116	5.54 (5.17)	11.1	0.29
heavy + mild ECMF Pd-TNTA	18.00	14.2	201	11.17 (8.96)	14.1	0.21

[a] Details of the electrochemically active surface area (EASA) measurements are found in Figure S8 in the Supporting Information. [b] Mass-specific peak current (the j_p^{m} values in round brackets refer to mass-specific current densities normalized against the as-deposited Pd-TNTA sample metal loading).

 © 2012 Wiley-VCH Verlag GmbH & Co. KGaA, Weinheim

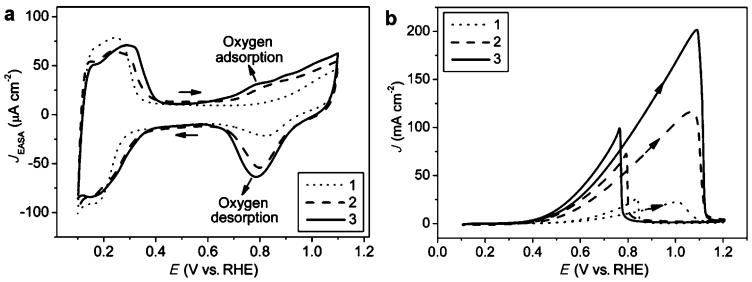

Figure 2. Cyclic voltammograms of TNTAs with deposited Pd recorded in a) 0.1 M $HClO_4$ and b) 2 M KOH with 10 wt% EtOH. Scan rate: 50 $mV s^{-1}$. Curve 1: TNTA-Pd as deposited. Curve 2: TNTA-Pd after heavy ECMF. Curve 3: TNTA-Pd after heavy and mild ECMF.

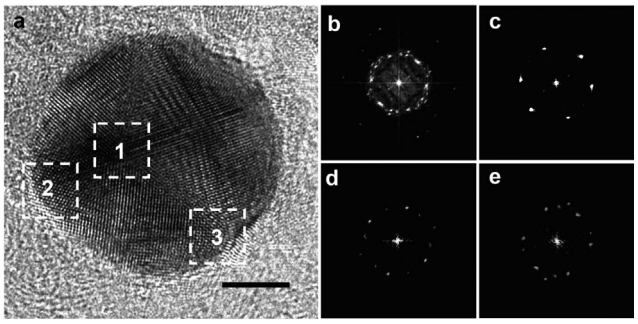

Figure 3. a) HRTEM image of a palladium multiple twinned particle removed from the TNTA after the heavy ECMF post-treatment (scale bar = 5 nm). b) Fourier transform (FT) patterns of the whole Pd particle. c–e) Selected-area FT patterns taken from zones 1, 2, and 3 in (a), respectively.

was also supported by a sequence of HRTEM pictures, taken at different tilting angles (Figure S13). MTPs have an enhanced catalytic activity relative to non-twinned NPs.[18] CV recorded in 0.1 M $HClO_4$ (Figure 2a, curve 2) showed that the oxygen adsorption/desorption current density at 0.8 V (vs. RHE) increases as compared to the as-deposited sample (Figure 2a, curve 1). Such evidence is consistent with a higher density of low-coordinated Pd atoms on the NP surface.[13,19] Accordingly, we think that the much higher ethanol electro-oxidation activity (shown in Table 1) originates from the combination of milling, formation of MTPs, and generation of high-index facets.

Applying the heavy ECMF procedure (Figure 1B) for more than 1080 s resulted in a further metal loss, which is detrimental to the catalytic performance. Consequently, we performed a milder ECMF sequence for further reduction of the particle size, which gave a higher density of low-coordinated Pd surface atoms with limited metal loss.

A mild ECMF post-deposition treatment with a frequency of 0.025 Hz for 3 h between +3.35 and −0.75 V (vs. RHE) has been found to be an appropriate route to size down the particles from 14 to 7 nm (Figure 1c) with a metal loss of 14%. Moreover, the reduction of the metal loading was paid back by a twofold increase in the peak current density as compared to the previous stage of the procedure (Table 1).

Low-magnification transmission electron microscopy (TEM) pictures (Figure 4a) showed the homogeneous distribution of the Pd NPs on the titania nanotubes. Small NPs have also been found in the process electrolyte (Figure 4b), allowing us to conclude that at least a fraction of the metal loss does not occur by dissolution, but simply because a limited part of the NPs unfasten from the TNTA surface. The size of the particles dispersed in the electrolyte was around 4 nm, suggesting that the present method could be a new and exciting route to the synthesis of free-standing Pd NPs.

HRTEM analysis of the TNTA-supported NPs after the ECMF post-deposition treatment, showed the existence of both high-index facets and twins. The acquisition of HRTEM images at a different focus allowed the assignment of the

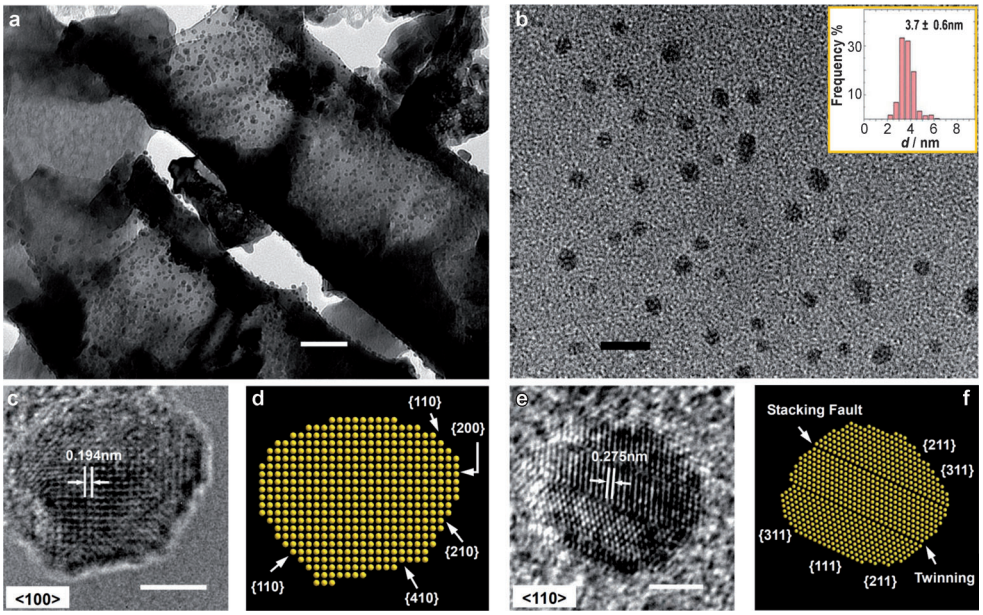

Figure 4. a) TEM image of the Pd-loaded TNTA electrode after heavy and mild ECMF (scale bar = 50 nm). b) Pd nanoparticles found in the electrolyte after heavy and mild ECMF (scale bar = 35 nm). c) HRTEM image (scale bar = 2 nm) and d) atomic models with face assignment of the TNTA-supported Pd nanoparticle along the ⟨100⟩ direction. e) HRTEM image (scale bar = 2 nm) and f) face assignment of the TNTA-supported Pd nanoparticles along the ⟨110⟩ direction.

© 2012 Wiley-VCH Verlag GmbH & Co. KGaA, Weinheim

surface structure. Figure 4c and e, according to the derived atomic models (Figure 4d and f), show the presence of high-index facets {210} and {410} along the ⟨100⟩ direction, and {211} and {311} facets along the <110> direction, respectively (a detailed analysis is given in Figures S14 and S15 in the Supporting Information). Along the <110> direction one may also notice the presence of twins and stacking faults. A CV study in 0.1M $HClO_4$ showed a remarkable enhancement of the oxygen adsorption/desorption at potentials lower than 0.8 V (vs. RHE), confirming a further increase in the density of low-coordinated surface atoms (Figure 2a, curve 3). Cyclic voltammetry using an ethanol-containing electrolyte showed a peak current density of 201 $mA\,cm^{-2}$ (Figure 2b, curve 3), corresponding to a mass-specific activity for Pd of 11167 $A\,g^{-1}$. Normalization of the activity to the initial metal loading gave instead a peak of 8965 $A\,g^{-1}$. Both values are remarkably higher than the highest reported value (3600 $A\,g^{-1}$)[20] determined under comparable conditions. The onset potential for the oxidation of ethanol was 0.21 V (vs. RHE), that is, 0.17 V more negative than the potential obtained for the as-deposited sample. Such data suggest that the application of the material developed in this work has a great potential for increasing the energy efficiency of direct ethanol fuel cells (DEFCs) as well as the hydrogen production by aqueous ethanol electrolysis.[3]

The stability of the catalyst has been verified by chronoamperomety (see Figure S10 in the Supporting Information), showing that the ECMF NPs are capable of delivering much higher EASA normalized current densities as compared to Pd NPs supported on carbon black with a similar metal loading.

The overall metal loading loss for the complete ECMF post-deposition treatment was 20% which resulted in a much higher mass-specific catalytic activity of Pd. The effectiveness of the technique is ascribed to the flexibility in the material characteristic selection, namely the metal loading, active surface area, and surface structure. In addition, the performances of practical nanocatalysts usually degrade because of the Ostwald ripening, that is, large particles grow at the expense of dissolved small particles. ECMF has a great potential to regenerate such deactivated catalysts, because it can be used for in situ reduction of the size of supported NPs without remarkable loss of metal.

Experimental Section

TNTAs have been synthesized by anodization at 60 V for one hour at room temperature in a solution of ethylene glycol containing 0.5 wt% of NH_4F. The TNTAs are then annealed by heating up to 400°C and are stable for 30 minutes.

Palladium nanoparticles have been deposited onto the TNTAs by sequential chemical bath deposition (S-CBD). The titania disk was immerged in beaker A containing $PdCl_2$ (0.3 g) and 0.7 mL of HCl (37%) and 1 mL of ethylene glycol in 50 mL of water for 30 s. The sample was then washed in pure water (beaker B). The reduction of the palladium salt adsorbed on the titania disk was obtained in beaker C, containing $NaBH_4$ (1 g) dissolved in 50 mL of deionized water. The sample was then washed in pure water (beaker D). The whole sequence was repeated ten times. The color of the sample after the deposition turned from light blue of the TNTA prior to the deposition to light black. Finally, the as-prepared samples were dried in a N_2 stream.

Post-treatment experiments have been carried out with a Princeton 2273A potentiostat/galvanostat with a three-electrode cell arrangement. A saturated calomel reference electrode (SCE) and a glassy carbon rod (diameter (Φ) = 1/4 inch) electrode were used as reference and counter electrodes, respectively. The electrolyte was a 2M KOH water solution. Prior to the experiments the electrolyte was purged with high-purity N_2. The electrochemical potentials were measured versus the RHE. The heavy ECMF post-deposition treatment required a palladium oxidation at 4.55 V (vs. RHE) for 180 s, followed by the reduction of the Pd oxide at −1.95 V (vs. RHE) for 180 s. The whole sequence was repeated three times (1080 s). Instead, the mild ECMF post-deposition treatment required a palladium oxidation and reduction with a frequency of 0.025 Hz for 10800 s between +3.35 and −0.75 V (vs. RHE).

A sample of palladium deposited on carbon black (Vulcan XC-72) was prepared for comparison with palladium-deposited TNTA samples. Vulcan XC-72 (5.94 g) was sonicated for 20 minutes in a 500 mL three-necked round-bottomed flask containing 250 mL of ethylene glycol. The resulting dispersion was added dropwise and under stirring with 50 mL of a water solution containing 0.6 g (3.38 mmol) $PdCl_2$ and 6 mL of HCl (37% w:w). After addition of the Pd-containing solution, 10 mL of a water solution containing 5.1 g NaOH were introduced into the reactor. The resulting mixture was then heated up to 140°C in nitrogen for 3 h. After cooling to room temperature, the formed solid was filtered off, washed, and neutralized with distilled water. The final product was dried at 40°C in vacuum to constant weight. The Pd content assessed by inductively coupled plasma mass spectrometry (ICP-MS) analysis was 5.2 wt.%.

Received: May 9, 2012
Published online: July 13, 2012

Keywords: electrocatalysis · electrochemistry · green chemistry · nanoparticles · palladium

[1] A. T. Bell, *Science* **2003**, *299*, 1688–1691.
[2] Y. M. Li, G. A. Somorjai, *Nano Lett.* **2010**, *10*, 2289–2295.
[3] V. Bambagioni, M. Bevilacqua, C. Bianchini, J. Filippi, A. Lavacchi, A. Marchionni, F. Vizza, P. K. Shen, *ChemSusChem* **2010**, *3*, 851–855.
[4] C. Bianchini, P. K. Shen, *Chem. Rev.* **2009**, *109*, 4183–4206.
[5] G. Cui, S. Song, P. K. Shen, A. Kowal, C. Bianchini, *J. Phys. Chem. C* **2009**, *113*, 15639–15642.
[6] L. Q. Wang, V. Bambagioni, M. Bevilacqua, C. Bianchini, J. Filippi, A. Lavacchi, A. Marchionni, F. Vizza, X. Fang, P. K. Shen, *J. Power Sources* **2010**, *195*, 8036–8043.
[7] N. Tian, Z. Y. Zhou, S. G. Sun, *J. Phys. Chem. C* **2008**, *112*, 19801–19817.
[8] Z. Y. Zhou, N. Tian, J. T. Li, I. Broadwell, S. G. Sun, *Chem. Soc. Rev.* **2011**, *40*, 4167–4185.
[9] F. Lu, Y. Zhang, L. H. Zhang, Y. G. Zhang, J. X. Wang, R. R. Adzic, E. A. Stach, O. Gang, *J. Am. Chem. Soc.* **2011**, *133*, 18074–18077.
[10] X. Q. Huang, Z. P. Zhao, J. M. Fan, Y. M. Tan, N. F. Zheng, *J. Am. Chem. Soc.* **2011**, *133*, 4718–4721.
[11] N. Tian, Z. Y. Zhou, S. G. Sun, Y. Ding, Z. L. Wang, *Science* **2007**, *316*, 732–735.
[12] T. Yu, D. Y. Kim, H. Zhang, Y. N. Xia, *Angew. Chem.* **2011**, *123*, 2825–2829; *Angew. Chem. Int. Ed.* **2011**, *50*, 2773–2777.
[13] N. Tian, Z. Y. Zhou, N. F. Yu, L. Y. Wang, S. G. Sun, *J. Am. Chem. Soc.* **2010**, *132*, 7580–7581.
[14] Z. Y. Zhou, Z. Z. Huang, D. J. Chen, Q. Wang, N. Tian, S. G. Sun, *Angew. Chem.* **2010**, *122*, 421–424; *Angew. Chem. Int. Ed.* **2010**, *49*, 411–414.

 © 2012 Wiley-VCH Verlag GmbH & Co. KGaA, Weinheim

[15] M. Grdeń, M. Łukaszewski, G. Jerkiewicz, A. Czerwiński, *Electrochim. Acta* **2008**, *53*, 7583 – 7598.
[16] P. Rodriguez, F. D. Tichelaar, M. T. M. Koper, A. I. Yanson, *J. Am. Chem. Soc.* **2011**, *133*, 17626 – 17629.
[17] A. I. Yanson, P. Rodriguez, N. Garcia-Araez, R. V. Mom, F. D. Tichelaar, M. T. M. Koper, *Angew. Chem.* **2011**, *123*, 6470 – 6474; *Angew. Chem. Int. Ed.* **2011**, *50*, 6346 – 6350.
[18] A. X. Yin, X. Q. Min, W. Zhu, H. S. Wu, Y. W. Zhang, C. H. Yan, *Chem. Commun.* **2012**, *48*, 543 – 545.
[19] A. Hitotsuyanagi, S. Kondo, M. Nakamura, N. Hoshi, *J. Electroanal. Chem.* **2011**, *657*, 123 – 127.
[20] V. Bambagioni, C. Bianchini, J. Filippi, W. Oberhauser, A. Marchionni, F. Vizza, R. Psaro, L. Sordelli, M. L. Foresti, M. Innocenti, *ChemSusChem* **2009**, *2*, 99 – 112.

 © 2012 Wiley-VCH Verlag GmbH & Co. KGaA, Weinheim